

Excitation energies in density functional theory: An evaluation and a diagnostic test

Michael J. G. Peach, Peter Benfield, Trygve Helgaker, and David J. Tozer

Citation: *The Journal of Chemical Physics* **128**, 044118 (2008); doi: 10.1063/1.2831900

View online: <http://dx.doi.org/10.1063/1.2831900>

View Table of Contents: <http://aip.scitation.org/toc/jcp/128/4>

Published by the [American Institute of Physics](#)

Articles you may be interested in

[Density-functional thermochemistry. III. The role of exact exchange](#)

The Journal of Chemical Physics **98**, 5648 (1998); 10.1063/1.464913

[Long-range charge-transfer excited states in time-dependent density functional theory require non-local exchange](#)

The Journal of Chemical Physics **119**, 2943 (2003); 10.1063/1.1590951

[Benchmarks for electronically excited states: CASPT2, CC2, CCSD, and CC3](#)

The Journal of Chemical Physics **128**, 134110 (2008); 10.1063/1.2889385

[A consistent and accurate ab initio parametrization of density functional dispersion correction \(DFT-D\) for the 94 elements H-Pu](#)

The Journal of Chemical Physics **132**, 154104 (2010); 10.1063/1.3382344

[Benchmarks for electronically excited states: Time-dependent density functional theory and density functional theory based multireference configuration interaction](#)

The Journal of Chemical Physics **129**, 104103 (2008); 10.1063/1.2973541

[Gaussian basis sets for use in correlated molecular calculations. I. The atoms boron through neon and hydrogen](#)

The Journal of Chemical Physics **90**, 1007 (1998); 10.1063/1.456153



Scilight

Sharp, quick summaries **illuminating**
the latest physics research

Sign up for **FREE!**

AIP
Publishing

Excitation energies in density functional theory: An evaluation and a diagnostic test

Michael J. G. Peach,¹ Peter Benfield,¹ Trygve Helgaker,^{1,2} and David J. Tozer^{1,a)}

¹*Department of Chemistry, University of Durham, South Road, Durham DH1 3LE, United Kingdom*

²*Centre for Theoretical and Computational Chemistry, Department of Chemistry, University of Oslo, P.O. Box 1033, Blindern, N-0315 Oslo, Norway*

(Received 14 November 2007; accepted 13 December 2007; published online 31 January 2008)

Electronic excitation energies are determined using the CAM-B3LYP Coulomb-attenuated functional [T. Yanai *et al.* Chem. Phys. Lett. **393**, 51 (2004)], together with a standard generalized gradient approximation (GGA) and hybrid functional. The degree of spatial overlap between the occupied and virtual orbitals involved in an excitation is measured using a quantity Λ , and the extent to which excitation energy errors correlate with Λ is quantified. For a set of 59 excitations of local, Rydberg, and intramolecular charge-transfer character in 18 theoretically challenging main-group molecules, CAM-B3LYP provides by far the best overall performance; no correlation is observed between excitation energy errors and Λ , reflecting the good quality, balanced description of all three categories of excitation. By contrast, a clear correlation is observed for the GGA and, to a lesser extent, the hybrid functional, allowing a simple diagnostic test to be proposed for judging the reliability of a general excitation from these functionals—when Λ falls below a prescribed threshold, excitations are likely to be in very significant error. The study highlights the ambiguous nature of the term “charge transfer,” providing insight into the observation that while many charge-transfer excitations are poorly described by GGA and hybrid functionals, others are accurately reproduced. © 2008 American Institute of Physics. [DOI: 10.1063/1.2831900]

I. INTRODUCTION AND BACKGROUND

Time-dependent density functional theory (TDDFT),^{1–4} in the adiabatic approximation,⁴ is extensively used for the calculation of electronic excitation energies. For real orbitals, the excitation energies are obtained as solutions of the generalized eigenvalue problem

$$\begin{pmatrix} \mathbf{A} & \mathbf{B} \\ \mathbf{B} & \mathbf{A} \end{pmatrix} \begin{pmatrix} \mathbf{X} \\ \mathbf{Y} \end{pmatrix} = \omega \begin{pmatrix} \mathbf{1} & \mathbf{0} \\ \mathbf{0} & -\mathbf{1} \end{pmatrix} \begin{pmatrix} \mathbf{X} \\ \mathbf{Y} \end{pmatrix}, \quad (1)$$

where the form of the matrices \mathbf{A} and \mathbf{B} is given in Refs. 3 and 5. For conventional generalized gradient approximation⁶ (GGA) and hybrid⁷ functionals, it is well established that local excitations are generally accurate to within a few tenths of an eV, whereas Rydberg excitations are significantly underestimated. The latter arises due to the incorrect asymptotic behavior of the exchange-correlation contribution to the Kohn–Sham equations⁸ and can be repaired using an asymptotic correction.^{9–12}

In recent years, many studies have also highlighted a significant underestimation of low-lying TDDFT excitation energies associated with significant charge transfer (CT),^{13–23} errors can be of the order of several eV and are not reduced by an asymptotic correction. The situation is complicated by the fact that for some molecules, CT excitations are accurately reproduced.^{24–26} In practical calculations, it can

therefore be difficult to judge the reliability of a TDDFT CT excitation.

The origin of the TDDFT CT error has been widely discussed.^{27–31} Of particular relevance to the present study is the analysis of Dreuw *et al.*,²⁷ who considered the intermolecular CT excitation from an occupied orbital on one molecule to a virtual orbital on another molecule. At infinite intermolecular separation, there is no spatial overlap between these two orbitals and so, for local functionals such as GGA, matrix \mathbf{A} in Eq. (1) reduces to a diagonal matrix of Kohn–Sham orbital energy differences, while $\mathbf{B} = \mathbf{0}$. The CT excitation energy is therefore given simply by the orbital energy difference. From Ref. 28, this quantity underestimates the experimental excitation energy by approximately the average of the integer discontinuities³² of the two molecules, which is of the order of several eV. Conventional hybrid functionals only partly fix the problem.

One approach that shows promise for improving the accuracy of both Rydberg and CT excitations while maintaining good quality local excitations is to partition the $1/r_{12}$ operator in the exchange term into short- and long-range components.^{33–38} Short-range exchange is then treated primarily using a local functional; long-range exchange is treated primarily using exact orbital exchange. For example, the Coulomb-attenuated CAM-B3LYP (Ref. 39) functional contains just 19% exact exchange at short range (like a conventional hybrid) but 65% at long range. It yields improved Rydberg excitations in small molecules^{40,41} and significantly improved CT excitations in a model dipeptide^{39,41} and in an asymptotic intermolecular complex.⁴² CT excitations that are

^{a)}FAX: +44-191-384-4737. Electronic mail: d.j.tozer@durham.ac.uk.

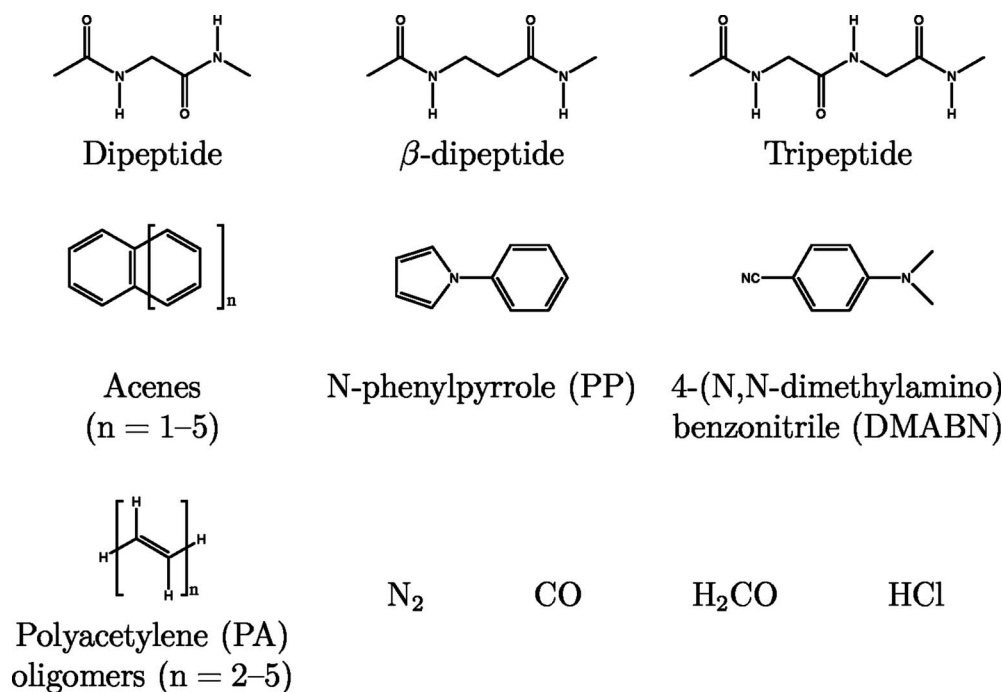


FIG. 1. Molecules considered in this study.

well represented using conventional functionals can, however, become slightly less accurate.⁴¹ For other relevant investigations, see Refs. 43–48.

The present study has two aims. First, we provide an extensive assessment of the quality of TDDFT excitation energies from selected GGA, hybrid, and Coulomb-attenuated functionals. A wide range of excitations in main-group molecules are considered, comprising local, Rydberg, and intramolecular CT. Following Refs. 27 and 28—which highlight the large errors that can occur in CT excitations when there is no spatial orbital overlap—we then consider the influence of overlap on a *general* excitation. Specifically, we quantify the extent to which excitation energy errors—for local, Rydberg, and intramolecular CT excitations—correlate with the spatial overlap between the occupied and virtual orbitals involved in the excitations for all three categories of functional. The results are intuitive and insightful. They lead us to propose a simple diagnostic test that can highlight when an excitation is likely to be particularly poor for GGA and hybrid functionals, enabling us to understand why some CT excitations are accurately reproduced with these functionals.

We commence in Sec. II by listing the molecules considered, summarizing the details of the excitations and presenting computational details. The accuracy of the TDDFT excitations is quantified in Sec. III. The relationship between excitation energy error and spatial orbital overlap is investigated in Sec. IV, and the diagnostic test is proposed. Conclusions are presented in Sec. V.

II. MOLECULES, EXCITATIONS, AND COMPUTATIONAL DETAILS

Figure 1 lists the molecules considered in this study. They were chosen to include a wide range of excitations,

many of which have been shown to be a challenge for TD-DFT. Table I lists the specific singlet excitations of interest. Those assigned to be of Rydberg or charge-transfer character in earlier studies (see below) are labeled R and CT, respectively. All other excitations are termed local excitations and are labeled L.

The first molecule is the model dipeptide of Ref. 49. This was one of the first highlighted cases where conventional functionals exhibit a large CT error.¹³ The notations n_i , π_i , and π_i^* , in Table I, refer to the nonbonding, π , and π^* orbitals on carbonyl group i , where $i=1$ or 2. The $n_1 \rightarrow \pi_2^*$ and $\pi_1 \rightarrow \pi_2^*$ excitations are therefore excitations from one carbonyl to another and are CT in character. The excitations $n_1 \rightarrow \pi_1^*$ and $n_2 \rightarrow \pi_2^*$ are local excitations, as the transitions involve only one carbonyl group. The next two molecules are a longer chain β -dipeptide and tripeptide, from Ref. 49, which have not previously been studied using TDDFT; the same notation is used. The larger distances between the carbonyl groups mean that the CT errors from conventional functionals are expected to be even more significant for these systems. Next is a series of linear condensed acenes of increasing length, as considered in Ref. 50. As noted in this earlier work, the ${}^1B_{2u}$ excitation is particularly problematic for TDDFT, and the ordering of the ${}^1B_{2u}$ and ${}^1B_{3u}$ states can be incorrect. The next two molecules are *N*-phenylpyrrole (PP), widely studied^{23,51} due to its significant photophysical properties, and 4-(*N,N*-dimethylamino)benzonitrile (DMABN), which is of interest due to its dual fluorescence. DMABN is an example of a system where conventional functionals provide a good description of the CT excitation²⁴—insight into this observation is provided in Sec. IV. The next four molecules are polyacetylene (PA) oligomers, as investigated recently in Ref. 52; we consider the lowest dipole-allowed transition. The final four molecules

TABLE I. TDDFT excitation energies and reference values, in eV.

Molecule	Excitation	Type	PBE	B3LYP	CAM-B3LYP	Ref.
Dipeptide	$n_1 \rightarrow \pi_2^*$	CT	4.61	6.31	7.84	8.07 ^a
	$\pi_1 \rightarrow \pi_2^*$	CT	5.16	6.15	7.00	7.18 ^a
	$n_1 \rightarrow \pi_1^*$	L	5.35	5.55	5.68	5.62 ^a
	$n_2 \rightarrow \pi_2^*$	L	5.67	5.77	5.92	5.79 ^a
β -dipeptide	$n_1 \rightarrow \pi_2^*$	CT	4.78	7.26	8.38	9.13 ^a
	$\pi_1 \rightarrow \pi_2^*$	CT	5.32	7.20	8.01	7.99 ^a
	$n_1 \rightarrow \pi_1^*$	L	5.38	5.66	5.67	5.40 ^a
	$n_2 \rightarrow \pi_2^*$	L	5.41	5.56	5.76	5.10 ^a
Tripeptide	$\pi_1 \rightarrow \pi_2^*$	CT	5.18	6.27	6.98	7.01 ^a
	$\pi_2 \rightarrow \pi_2^*$	CT	5.51	6.60	7.69	7.39 ^a
	$\pi_1 \rightarrow \pi_3^*$	CT	4.76	6.06	8.51	8.74 ^a
	$n_1 \rightarrow \pi_3^*$	CT	4.26	6.12	8.67	9.30 ^a
	$n_2 \rightarrow \pi_3^*$	CT	5.16	6.83	8.25	8.33 ^a
	$n_1 \rightarrow \pi_1^*$	CT	4.61	6.33	7.78	8.12 ^a
	$n_1 \rightarrow \pi_1^*$	L	5.36	5.57	5.72	5.74 ^a
	$n_2 \rightarrow \pi_2^*$	L	5.58	5.74	5.93	5.61 ^a
Acene ($n=1$)	$n_3 \rightarrow \pi_3^*$	L	5.74	5.88	6.00	5.91 ^b
	$^1B_{2u}$	L	4.11	4.38	4.67	4.88 ^b
Acene ($n=2$)	$^1B_{3u}$	L	4.27	4.47	4.62	4.46 ^b
	$^1B_{2u}$	L	2.94	3.21	3.53	3.69 ^b
Acene ($n=3$)	$^1B_{3u}$	L	3.64	3.86	4.04	3.89 ^b
	$^1B_{2u}$	L	2.17	2.43	2.76	2.90 ^b
Acene ($n=4$)	$^1B_{3u}$	L	3.24	3.47	3.65	3.52 ^b
	$^1B_{2u}$	L	1.63	1.89	2.22	2.35 ^b
Acene ($n=5$)	$^1B_{3u}$	L	2.96	3.21	3.39	3.27 ^b
	$^1B_{2u}$	L	1.23	1.48	1.82	1.95 ^b
PP	$^1B_{3u}$	L	2.76	3.01	3.21	3.09 ^b
	1^1B_2	L	4.33	4.76	5.06	4.85 ^c
	2^1A_1	L	4.61	4.96	5.12	5.13 ^c
	2^1B_2	CT	3.98	4.58	5.27	5.47 ^c
DMABN	3^1A_1	CT	3.90	4.64	5.92	5.94 ^c
	1B	L	4.02	4.44	4.72	4.25 ^d
	1A	CT	4.30	4.64	4.91	4.56 ^d
PA oligomer ($n=2$)	1B_u	L	5.74	5.88	6.04	5.92 ^e
PA oligomer ($n=3$)	1B_u	L	4.63	4.81	5.03	4.95 ^f
PA oligomer ($n=4$)	1B_u	L	3.93	4.13	4.39	4.41 ^g
PA oligomer ($n=5$)	1B_u	L	3.44	3.66	3.94	4.27 ^c
N_2	$^1\Pi_u$	R	11.67	12.01	12.44	13.24 ^h
	$^1\Sigma_u^+$	R	10.66	11.62	12.32	12.98 ^h
	$^1\Pi_u$	R	10.76	11.65	12.27	12.90 ^h
	$^1\Sigma_g^+$	R	10.41	11.24	11.80	12.20 ^h
	$^1\Delta_u$	L	10.08	9.72	9.68	10.27 ^h
	$^1\Sigma_u^-$	L	9.68	9.33	9.21	9.92 ^h
	$^1\Pi_g^-$	L	9.10	9.26	9.38	9.31 ^h
	$F^1\Sigma^+$	R	10.16	10.97	11.79	12.40 ⁱ
CO	$E^1\Pi$	R	9.45	10.19	10.90	11.53 ⁱ
	$C^1\Sigma^+$	R	9.40	10.13	10.80	11.40 ⁱ
	$B^1\Sigma^+$	R	9.09	9.80	10.37	10.78 ⁱ
	$D^1\Delta$	L	10.18	10.03	10.08	10.23 ⁱ
	$I^1\Sigma^-$	L	9.86	9.72	9.71	9.88 ⁱ
	$A^1\Pi$	L	8.24	8.39	8.47	8.51 ⁱ
	1A_2	R	7.43	8.16	8.87	9.22 ^j
H_2CO	1A_2	R	6.61	7.34	7.94	8.38 ^j
	1B_1	L	8.68	8.83	8.95	8.68 ^j
	1B_2	R	6.50	7.16	7.62	8.12 ^j
	1A_1	R	6.39	7.14	7.74	7.97 ^j
	1B_2	R	5.78	6.43	6.89	7.09 ^j
	1A_2	L	3.73	3.85	3.85	3.94 ^j
HCl	$^1\Pi$	CT	7.55	7.65	7.79	8.23 ^c

^aCASPT2, Ref. 49.^bCC2, Ref. 50.^cCC2, this work.^dGas-phase experiment, Ref. 67.^eGas-phase experiment, Ref. 68.^fGas-phase experiment, Ref. 69.^gGas-phase experiment, Ref. 70.^hGas-phase experiment, Ref. 71.ⁱGas-phase experiment, Refs. 59 and 72.^jGas phase experiment, Refs. 73 and 74.

are N₂, CO, H₂CO (see Ref. 9), and HCl (see Ref. 53), the first three of which allow the accuracy of Rydberg excitations to be assessed.

All calculations were performed using a locally modified development version of the DALTON program.⁵⁴ The TDDFT calculations were performed using the adiabatic approximation with three exchange-correlation functionals: the Perdew–Burke–Ernzerhof⁶ (PBE) GGA containing no exact orbital exchange, the Becke–3–Lee–Yang–Parr^{7,55–57} (B3LYP) hybrid functional containing a fixed amount (20%) of exact exchange, and the CAM-B3LYP (Ref. 39) Coulomb-attenuated functional containing 19% exact exchange at small r_{12} and 65% exact exchange at large r_{12} .

Calculations on the acenes were performed at B3LYP/TZVP geometries in order to allow comparison with the *ab initio* excitations of Grimme and Parac.⁵⁰ For the PA oligomers, CAM-B3LYP/6-31G* geometries were used⁵² due to their high-quality bond length alternation.^{52,58} For N₂ and CO, the experimental geometry of Ref. 59 was used. Calculations on all other molecules were performed at MP2/6-31G* geometries. All the geometries are available from Ref. 60.

All calculated excitation energies presented in this work are vertical values, determined with the cc-pVTZ basis set,⁶¹ except for N₂, CO, and H₂CO, where the *d*-aug-cc-pVTZ basis set⁶² is used due to the Rydberg character of some of the excitations (see Sec. III for a discussion of this point). For all the other molecules, we have confirmed where possible that the TDDFT results are relatively insensitive to the addition of diffuse functions to the basis—the excitation energies typically change by less than 0.1 eV in moving from cc-pVTZ to aug-cc-pVTZ.⁶³

The accuracy of the TDDFT excitation energies is quantified by comparing with reference values. Where gas-phase experimental data are available, we use these for the reference data. For the model peptides, complete active space with second-order perturbation theory^{64,65} (CASPT2) data is used. For the remaining molecules, second-order approximate coupled-cluster⁶⁶ (CC2) data is used. The CASPT2 and CC2 values were determined at the same geometry as the TDDFT calculations; all CC2 calculations performed in the present study use the cc-pVTZ basis set. Full details of the reference values are presented in Table I. The conclusions of this study are not dependent on this choice of geometry, basis set, and reference value; analogous observations are made when the computational details of the earlier studies are instead used.

III. FUNCTIONAL PERFORMANCE

Table I compares TDDFT excitation energies with reference values. First, consider the PBE GGA functional. Excitations of CT character are significantly underestimated; DMABN is the exception, consistent with Ref. 24. As anticipated, CT errors are largest for the tripeptide, with errors up to 5 eV. The Rydberg excitations in N₂, CO, and H₂CO exhibit the usual significant underestimation, with errors of several eV. These excitations exhibit an unacceptable dependence on the diffuseness of the basis set.⁸ To illustrate this,

we have performed additional calculations using a triply augmented basis, obtained by adding an extra shell of diffuse functions for each angular momentum, with exponents obtained from the geometric progression. All the Rydberg excitations are reduced by an average of 0.27 eV; the local excitations are unaffected by the additional functions.

Consistent with Ref. 50, the PBE ¹B_{2u} excitations in Table I are much too low in the acenes, with the ¹B_{2u}/¹B_{3u} state ordering incorrect for the $n=1$ case. The local excitation energies in PP are notably underestimated and the error for the PA oligomers increases as the chain lengthens. The remaining excitations are reasonably accurate. The poor overall performance of PBE is illustrated by the fact that of the 59 excitations considered, 25 have an error larger than 1 eV and 35 have a percentage error greater than 10%.

The introduction of a fixed amount of exact orbital exchange in B3LYP increases most excitation energies relative to PBE. It follows that CT excitations do improve, but they still remain too low (except for DMABN). The Rydberg excitations also improve and become less sensitive to the basis set—they reduce by an average of 0.1 eV (one-third of the PBE value) when the additional diffuse functions are added. The ¹B_{2u} and ¹B_{3u} states in the acenes both become more accurate, although the state ordering remains incorrect for $n=1$. The PP local excitations improve significantly. The PA oligomer excitations also improve, although the error remains large for the longer chains. The remaining excitations are reasonably accurate. Overall, 16 excitations have an error larger than 1 eV and 25 have a percentage error greater than 10%.

In moving to the Coulomb-attenuated CAM-B3LYP functional, there is a further increase in most excitation energies. For the CT excitations, the tendency to underestimate is eliminated; only two errors are now larger than 0.5 eV. The description of the Rydberg excitations is also improved compared to B3LYP, and the basis set sensitivity is further diminished—they reduce by an average of just 0.03 eV when the additional diffuse functions are added. The CAM-B3LYP Rydberg errors can still approach one eV, reflecting the fact that these excitations require 100% long-range exact orbital exchange, while CAM-B3LYP contains only 65%. This deficiency can be repaired with an asymptotic correction, as was done in Ref. 40.

The CAM-B3LYP description of the acene excitations is particularly good, with the state ordering now correct for all the systems. The functional also performs well for PP and the PA oligomers. The remaining excitations are reasonably accurate, although large errors remain for the $n_2 \rightarrow \pi_2^*$ excitation in the β -dipeptide and the ¹ Σ_u^- excitation in N₂. Overall, none of the excitations have an error larger than 1 eV and only two have a percentage error greater than 10%.

Table II lists the mean error (ME), mean absolute error (MAE), standard deviation (SD), and maximum positive and negative deviations, relative to reference values, according to excitation category; errors are defined as calculated minus reference. For local excitations, B3LYP is a clear improvement over PBE; CAM-B3LYP provides a similar MAE and

TABLE II. Mean error (ME), mean absolute error (MAE), standard deviation (SD), and maximum positive and negative deviations, in eV.

	PBE	B3LYP	CAM-B3LYP
Local			
ME	-0.31	-0.15	0.02
MAE	0.33	0.22	0.20
SD	0.27	0.26	0.27
Max(+)	0.31	0.46	0.66
Max(-)	-0.83	-0.61	-0.71
Rydberg			
ME	-1.84	-1.11	-0.50
MAE	1.84	1.11	0.50
SD	0.30	0.23	0.18
Max(+)	None	None	None
Max(-)	-2.24	-1.43	-0.80
Charge transfer			
ME	-2.60	-1.35	-0.18
MAE	2.60	1.36	0.27
SD	1.37	0.86	0.31
Max(+)	None	0.08	0.35
Max(-)	-5.04	-3.18	-0.75

SD to B3LYP, but the maximum errors are slightly larger. For both Rydberg and CT, the improvement from PBE to B3LYP to CAM-B3LYP is very clear.

An alternative way to fix the Rydberg excitations is to change the functional parametrization such that there is 100% exact orbital exchange at long range. This would also lead to accurate asymptotic intermolecular CT excitations since they too require 100% long-range exchange.^{27,42} To investigate the influence of this reparametrization on non-Rydberg excitations, we have applied the $\alpha=0.2$, $\beta=0.8$, $\mu=0.4 a_0$ functional (see Ref. 41) and the $\alpha=0.0$, $\beta=1.0$, $\mu=0.4 a_0$ functional to selected molecules in Table I. We find that the CT excitations can become significantly overestimated (see Ref. 41 for further discussion).

IV. CORRELATION BETWEEN ERROR AND ORBITAL OVERLAP

It is evident from Tables I and II that while all three functionals perform reasonably well for local excitations, there is a marked variation in the performance for Rydberg and CT. Following Refs. 27 and 28, we now consider whether this can be elaborated upon by quantifying the extent to which excitation energy errors correlate with the spatial overlap between the (unperturbed) occupied and virtual orbitals involved in the excitations.

For a given occupied orbital φ_i and virtual orbital φ_a , a natural measure of spatial overlap is the inner product of the moduli of the two orbitals,

$$O_{ia} = \langle |\varphi_i| | |\varphi_a| \rangle = \int |\varphi_i(\mathbf{r})| |\varphi_a(\mathbf{r})| d\mathbf{r}, \quad (2)$$

which can easily be evaluated using standard numerical integration schemes in TDDFT implementations; without the moduli, the integral would be trivially zero for all pairs. In practice, many occupied-virtual pairs contribute to a given

TDDFT excitation, and the contribution from each pair can be measured by

$$\kappa_{ia} = X_{ia} + Y_{ia}, \quad (3)$$

where X_{ia} and Y_{ia} are elements of the solution vectors of Eq. (1). This quantity (within a possible multiplicative constant) is commonly printed out in electronic structure programs for assignment purposes.

A measure of spatial overlap for a given excitation can therefore be obtained by weighting each inner product O_{ia} by some function $f(\kappa_{ia})$, and summing over all occupied-virtual pairs, suitably normalized. To avoid cancellations due to sign changes, we considered both $f(\kappa_{ia}) = |\kappa_{ia}|$ and $f(\kappa_{ia}) = \kappa_{ia}^2$. We evaluated the overlap measure for all the excitations in Table I, and although the two approaches yielded different absolute values for a given excitation, the trends were the same. We found that using $f(\kappa_{ia}) = \kappa_{ia}^2$ produced a wider range of overlap values, allowing excitations to be more readily distinguished. For the remainder of this study, we therefore measure the spatial overlap in a given excitation using the quantity

$$\Lambda = \frac{\sum_{i,a} \kappa_{ia}^2 O_{ia}}{\sum_{i,a} \kappa_{ia}^2}, \quad (4)$$

which takes the value $0 \leq \Lambda \leq 1$. A small value of Λ signifies a long-range excitation; a large value signifies a short-range excitation.

Figure 2 plots the error in the excitation energies in Table I against the associated Λ values for PBE, B3LYP, and CAM-B3LYP. Each point corresponds to a single excitation, with different symbols (and colors, online) for the three categories of excitation. The Λ values for individual excitations are available in the supplementary material, which is available through the EPAPS depository.⁷⁵

First, consider the PBE results in Fig. 2(a). The three categories of excitation are readily distinguished. The local excitations have a relatively large overlap, $0.45 \leq \Lambda \leq 0.89$, indicating that the occupied and virtual orbitals involved in the excitation occupy similar regions of space. This is to be expected for local excitations, where the degree of charge redistribution is small. By contrast, the Rydberg excitations have much smaller values, $0.08 \leq \Lambda \leq 0.27$, indicating only a minimal spatial overlap between the occupied and virtual orbitals. This is again to be expected due to the diffuse nature of the Rydberg orbitals. The CT excitations cover a surprisingly wide range of overlaps, from $\Lambda=0.06$ in the tripeptide to $\Lambda=0.72$ in DMABN. Figure 2(a) illustrates a clear correlation between the PBE excitation energy errors and Λ ; large errors are associated with small Λ and small errors are associated with large Λ . The correlation provides a simple explanation as to why the CT excitation in DMABN—unlike many CT excitations—is well described by PBE: The spatial overlap between the orbitals involved in the excitation is large.

Note that we do not explicitly consider intermolecular CT excitations between infinitely separated molecules in the present study. For such systems, the error in the excitation energy is approximately minus the average of the integer discontinuities of the two molecules.²⁸ The discontinuity can

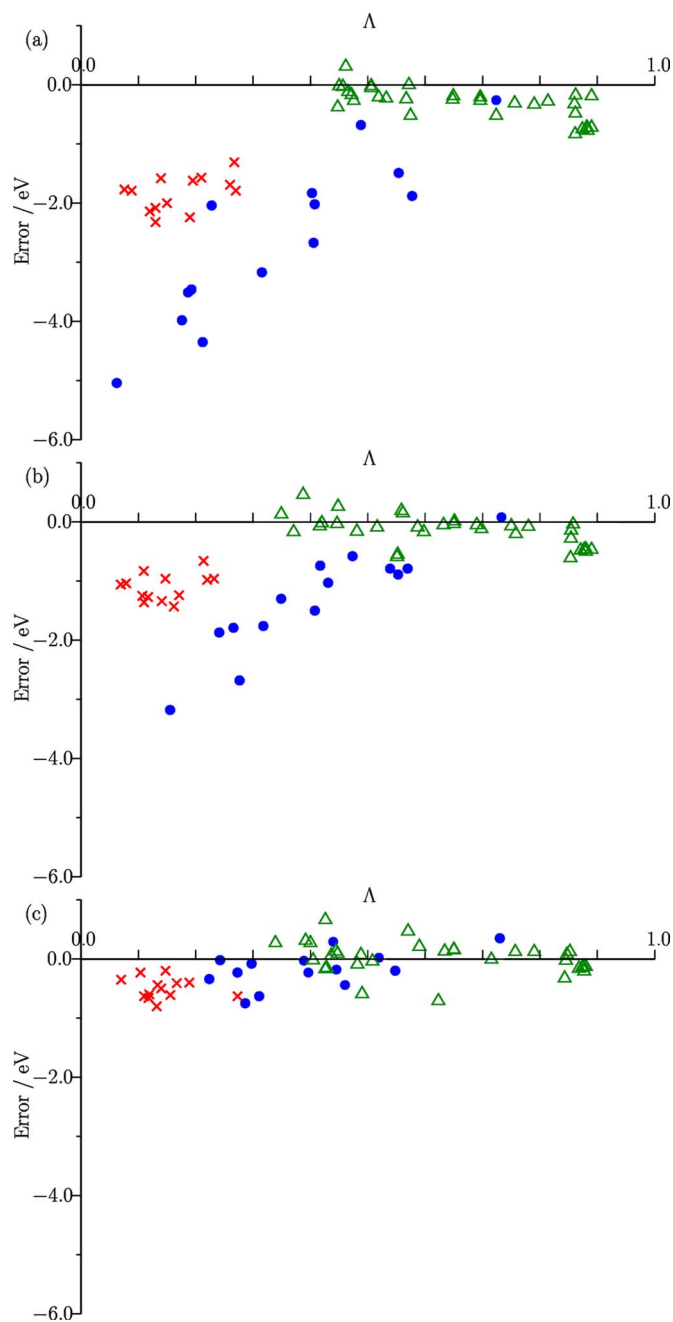


FIG. 2. (Color online) Excitation energy errors plotted against Λ [Eq. (4)] using (a) PBE, (b) B3LYP, and (c) CAM-B3LYP for local excitations (Δ), Rydberg excitations (\times), and CT excitations (\bullet).

be approximated as twice the system-dependent shift that must be introduced when semiempirical functionals are determined from high-quality potentials. It is apparent from the data in Table I of Ref. 76 that for typical pairs of molecules, this error is well in excess of -5 eV (see also the data in Ref. 28). Such excitations have $\Lambda=0$, and so the data points for intermolecular CT excitations between infinitely separated molecules would fit well with the CT data in Fig. 2(a).

In moving to B3LYP and CAM-B3LYP in Figs. 2(b) and 2(c), respectively, the excitation energy errors reduce according to the value of Λ . Those with large Λ , such as the local excitations and the DMABN CT excitation, do not change appreciably. With reducing Λ , however, the error reduction

becomes increasingly pronounced. For B3LYP, the correlation between excitation energy errors and Λ is still present but is less prominent than with PBE; the good quality DMABN CT excitation can again be attributed to the large Λ value. For CAM-B3LYP, the correlation has all but vanished, which is exactly what should be observed from a successful theoretical method. The reduction in correlation from PBE to B3LYP to CAM-B3LYP reflects the increased amounts of long-range, nonlocal exact orbital exchange in the three functionals.

Of the three functionals, CAM-B3LYP therefore provides by far the best overall description of the excitations, with essentially no correlation between errors and spatial orbital overlap, as measured by Λ . This functional is to be recommended for general excitation energy calculations. For PBE and B3LYP—and we expect similar observations for other GGAs and hybrids—the observed correlation between excitation energy errors and Λ leads us to propose a simple diagnostic test for judging the reliability of a given excitation: Following Figs. 2(a) and 2(b), a PBE excitation with $\Lambda < 0.4$ or a B3LYP excitation with $\Lambda < 0.3$ is likely to be in very significant error. The quantity Λ is not unique, and its diagnostic value is qualitative rather than quantitative. However, it captures the essential physics of the problem and may prove useful in practical calculations.

V. CONCLUSIONS

We have presented an extensive assessment of the performance of the PBE, B3LYP, and CAM-B3LYP exchange-correlation functionals for the calculation of local, Rydberg, and intramolecular CT excitation energies. We have subsequently quantified the extent to which excitation energy errors correlate with the spatial overlap between the occupied and virtual orbitals, as measured by the overlap quantity Λ in Eq. (4). The results reflect the differing amounts of long-range, nonlocal exact orbital exchange in the three functionals.

The CAM-B3LYP functional provides the best overall description of the excitation energies. Rydberg excitations remain in error, but can be improved through the application of an asymptotic correction.^{9–12,40} No correlation is observed between the CAM-B3LYP errors and Λ , reflecting the good quality, balanced description of all three categories of excitation. The functional is recommended for excitation energy calculations.

The PBE and, to a lesser extent, B3LYP functionals exhibit a clear correlation between excitation energy errors and Λ ; the errors increase as Λ reduces. This has led us to propose a simple diagnostic test for judging the reliability of a given excitation from these functionals: A PBE excitation with $\Lambda < 0.4$ or a B3LYP excitation with $\Lambda < 0.3$ is likely to be in very significant error. The quantity Λ is not unique, and its diagnostic value is qualitative rather than quantitative. However, it captures the essential physics of the problem and may prove useful in practical calculations. It can be trivially computed from quantities available in a regular TDDFT calculation and will be routinely available in the next release of the DALTON program.⁵⁴ Further investigation of this diagnos-

tic test, particularly to determine its applicability to non-main-group molecules, is required; we are presently considering excitations in transition metal complexes.

Finally, the results highlight the ambiguous nature of the term “charge transfer.” The CT excitations in Fig. 2 span a surprisingly wide range of Λ values. The smallest Λ values are, as expected, associated with the peptide systems; the largest value is associated with DMABN. The observed correlation of the errors with Λ provides a simple explanation as to why the dipeptide CT (small Λ) is poorly described by GGA and hybrid functionals,¹³ whereas the DMABN CT (large Λ) is well described.²⁴ It is inappropriate to say that these functionals fail to describe CT excitations. The degree of CT—in the sense of how much the occupied and virtual orbitals overlap—must be quantified using Λ or some related quantity before judgment can be made.

ACKNOWLEDGMENTS

The authors thank A.M. Teale, E.I. Tellgren, G.E. Scuseria, and E.N. Brothers for helpful discussions. D.J.T. and M.J.G.P. thank the EPSRC for studentship support. T.H. gratefully acknowledges the hospitality of the University of Durham while on Research Leave, 2006–2007, and funding from the Norwegian Research Council through a Strategic University Program in Quantum Chemistry (Grant No. 154011/420) and through a grant of computer time from the Program for Supercomputing.

¹E. Runge and E. K. U. Gross, Phys. Rev. Lett. **52**, 997 (1984).

²E. K. U. Gross, C. A. Ullrich, and U. J. Gossmann, in *Density Functional Theory*, NATO Advanced Studies Institute, Series B: Physics, edited by E. K. U. Gross and R. M. Dreizler (Plenum, New York, 1994), p. 149.

³M. E. Casida, in *Recent Advances in Density Functional Methods, Part I*, edited by D. P. Chong (Singapore, World Scientific, 1995), p. 155.

⁴M. A. L. Marques and E. K. U. Gross, Annu. Rev. Phys. Chem. **55**, 427 (2004).

⁵R. Bauernschmitt and R. Ahlrichs, Chem. Phys. Lett. **256**, 454 (1996).

⁶J. P. Perdew, K. Burke, and M. Ernzerhof, Phys. Rev. Lett. **77**, 3865 (1996).

⁷A. D. Becke, J. Chem. Phys. **98**, 5648 (1993).

⁸M. E. Casida, C. Jamorski, K. C. Casida, and D. R. Salahub, J. Chem. Phys. **108**, 4439 (1998).

⁹D. J. Tozer and N. C. Handy, J. Chem. Phys. **109**, 10180 (1998).

¹⁰M. E. Casida, K. C. Casida, and D. R. Salahub, Int. J. Quantum Chem. **70**, 933 (1998).

¹¹M. J. Allen and D. J. Tozer, J. Chem. Phys. **113**, 5185 (2000).

¹²M. Grüning, O. V. Gritsenko, S. J. A. van Gisbergen, and E. J. Baerends, J. Chem. Phys. **114**, 652 (2001).

¹³D. J. Tozer, R. D. Amos, N. C. Handy, B. O. Roos, and L. Serrano-Andrés, Mol. Phys. **97**, 859 (1999).

¹⁴J. Fabian, Theor. Chem. Acc. **106**, 199 (2001).

¹⁵A. Dreuw, G. Fleming, and M. Head-Gordon, J. Phys. Chem. B **107**, 6500 (2003).

¹⁶A. Dreuw, G. R. Fleming, and M. Head-Gordon, Phys. Chem. Chem. Phys. **5**, 3247 (2003).

¹⁷M.-S. Liao, Y. Lu, and S. Scheiner, J. Comput. Chem. **24**, 623 (2003).

¹⁸A. L. Sobolewski and W. Domcke, Chem. Phys. **294**, 73 (2003).

¹⁹A. Dreuw and M. Head-Gordon, J. Am. Chem. Soc. **126**, 4007 (2004).

²⁰S. Anand and H. B. Schlegel, Mol. Phys. **104**, 933 (2006).

²¹E. Fabiano, F. Della Sala, G. Barbarella, S. Lattante, M. Anni, G. Sotgiu, C. Hättig, R. Cingolani, and G. Gigli, J. Phys. Chem. B **110**, 18651 (2006).

²²E. Perpete, J. Preat, J.-M. Andre, and D. Jacquemin, J. Phys. Chem. A **110**, 5629 (2006).

²³X. Xu, Z. Cao, and Q. Zhang, J. Phys. Chem. A **110**, 1740 (2006).

²⁴C. Jamorski, J. B. Foresman, C. Thilgen, and H.-P. Lüthi, J. Chem. Phys. **116**, 8761 (2002).

²⁵D. Rappoport and F. Furche, J. Am. Chem. Soc. **126**, 1277 (2004).

²⁶D. Jacquemin, M. Bouhy, and E. A. Perpète, J. Chem. Phys. **124**, 204321 (2006).

²⁷A. Dreuw, J. L. Weisman, and M. Head-Gordon, J. Chem. Phys. **119**, 2943 (2003).

²⁸D. J. Tozer, J. Chem. Phys. **119**, 12697 (2003).

²⁹O. Gritsenko and E. J. Baerends, J. Chem. Phys. **121**, 655 (2004).

³⁰N. T. Maitra, J. Chem. Phys. **122**, 234104 (2005).

³¹J. Neugebauer, O. Gritsenko, and E. J. Baerends, J. Chem. Phys. **124**, 214102 (2006).

³²J. P. Perdew, R. G. Parr, M. Levy, and J. L. Balduz, Phys. Rev. Lett. **49**, 1691 (1982).

³³A. Savin, in *Recent Developments and Applications of Modern Density Functional Theory*, edited by J. M. Seminario (Elsevier, Amsterdam, 1996), p. 327.

³⁴P. M. W. Gill, R. D. Adamson, and J. A. Pople, Mol. Phys. **88**, 1005 (1996).

³⁵T. Leininger, H. Stoll, H.-J. Werner, and A. Savin, Chem. Phys. Lett. **275**, 151 (1997).

³⁶H. Iikura, T. Tsuneda, T. Yanai, and K. Hirao, J. Chem. Phys. **115**, 3540 (2001).

³⁷I. C. Gerber and J. G. Angyan, Chem. Phys. Lett. **415**, 100 (2005).

³⁸O. A. Vydrov, J. Heyd, A. V. Krukau, and G. E. Scuseria, J. Chem. Phys. **125**, 074106 (2006).

³⁹T. Yanai, D. P. Tew, and N. C. Handy, Chem. Phys. Lett. **393**, 51 (2004).

⁴⁰T. Yanai, R. J. Harrison, and N. C. Handy, Mol. Phys. **103**, 413 (2005).

⁴¹M. J. G. Peach, A. J. Cohen, and D. J. Tozer, Phys. Chem. Chem. Phys. **8**, 4543 (2006).

⁴²M. J. G. Peach, T. Helgaker, P. Salek, T. W. Keal, O. B. Lutnæs, D. J. Tozer, and N. C. Handy, Phys. Chem. Chem. Phys. **8**, 558 (2006).

⁴³Y. Tawada, T. Tsuneda, S. Yanagisawa, T. Yanai, and K. Hirao, J. Chem. Phys. **120**, 8425 (2004).

⁴⁴R. Kobayashi and R. D. Amos, Chem. Phys. Lett. **420**, 106 (2006).

⁴⁵M. Chiba, T. Tsuneda, and K. Hirao, J. Chem. Phys. **124**, 144106 (2006).

⁴⁶P. N. Day, K. A. Nguyen, and R. Pachter, J. Chem. Phys. **125**, 094103 (2006).

⁴⁷D. Jacquemin, E. A. Perpète, O. A. Vydrov, G. E. Scuseria, and C. Adamo, J. Chem. Phys. **127**, 094102 (2007).

⁴⁸K. A. Nguyen, P. N. Day, and R. Pachter, J. Chem. Phys. **126**, 094303 (2007).

⁴⁹L. Serrano-Andrés and M. Fulscher, J. Am. Chem. Soc. **120**, 10912 (1998).

⁵⁰S. Grimme and M. Parac, ChemPhysChem **4**, 292 (2003).

⁵¹B. Proppe, M. Merchán, and L. Serrano-Andrés, J. Phys. Chem. A **104**, 1608 (2000).

⁵²M. J. G. Peach, E. I. Tellgren, P. Salek, T. Helgaker, and D. J. Tozer, J. Phys. Chem. A **111**, 11930 (2007).

⁵³C. Hu, O. Sugino, and Y. Miyamoto, Phys. Rev. A **74**, 032508 (2006).

⁵⁴DALTON, Release 2.0, a molecular electronic structure program, 2005 (see <http://www.kjemi.uio.no/software/dalton/dalton.html>).

⁵⁵C. Lee, W. Yang, and R. G. Parr, Phys. Rev. B **37**, 785 (1988).

⁵⁶S. H. Vosko, L. Wilk, and M. Nusair, Can. J. Phys. **58**, 1200 (1980).

⁵⁷P. J. Stephens, F. J. Devlin, C. F. Chabalowski, and M. J. Frisch, J. Phys. Chem. **98**, 11623 (1994).

⁵⁸D. Jacquemin, E. A. Perpete, G. Scalmani, M. J. Frisch, R. Kobayashi, and C. Adamo, J. Chem. Phys. **126**, 144105 (2007).

⁵⁹K. P. Huber and G. Herzberg, *Constants of Diatomic Molecules*, Molecular Spectra and Molecular Structure Vol. 4 (Van Nostrand, New York, 1979).

⁶⁰See <http://www.dur.ac.uk/d.j.tozer/benchmark.html> for more information.

⁶¹T. H. Dunning, Jr., J. Chem. Phys. **90**, 1007 (1989).

⁶²D. E. Woon and T. H. Dunning, Jr., J. Chem. Phys. **100**, 2975 (1994).

⁶³R. A. Kendall, T. H. Dunning, Jr., and R. J. Harrison, J. Chem. Phys. **96**, 6796 (1992).

⁶⁴K. Andersson, P.-Å. Malmqvist, B. O. Roos, A. J. Sadlej, and K. Wolinski, J. Phys. Chem. **94**, 5483 (1990).

⁶⁵K. Andersson, P.-Å. Malmqvist, and B. O. Roos, J. Chem. Phys. **96**, 1218 (1992).

⁶⁶O. Christiansen, H. Koch, and P. Jørgensen, Chem. Phys. Lett. **243**, 409 (1995).

- ⁶⁷C. Bulliard, M. Allan, G. Wirtz, E. Haselbach, K. Zachariasse, N. Detzer, and S. Grimme, *J. Phys. Chem. A* **103**, 7766 (1999).
- ⁶⁸R. McDiarmid, *J. Chem. Phys.* **64**, 514 (1976).
- ⁶⁹W. M. Flicker, O. A. Mosher, and A. Kuppermann, *Chem. Phys. Lett.* **45**, 492 (1977).
- ⁷⁰D. G. Leopold, R. D. Pendley, J. L. Roebber, R. J. Hemley, and V. Vaida, *J. Chem. Phys.* **81**, 4218 (1984).
- ⁷¹S. B. Ben-Shlomo and U. Kaldor, *J. Chem. Phys.* **92**, 3680 (1990).
- ⁷²E. S. Nielsen, P. Jørgensen, and J. Oddershede, *J. Chem. Phys.* **73**, 6238 (1980).
- ⁷³D. J. Clouthier and D. A. Ramsay, *Annu. Rev. Phys. Chem.* **34**, 31 (1983).
- ⁷⁴S. Taylor, D. G. Wilden, and J. Comer, *Chem. Phys.* **70**, 291 (1982).
- ⁷⁵See EPAPS Document No. E-JCPSA6-128-029805 for the Λ values corresponding to the excitations in Table II for each of the functionals considered. This document can be reached through a direct link in the online article's HTML reference section or via the EPAPS homepage (<http://www.aip.org/pubservs/epaps.html>).
- ⁷⁶D. J. Tozer and N. C. Handy, *Mol. Phys.* **101**, 2669 (2003).